BNL-221555-2021-JAAM

Simulations of coherent scattering experiments at storage ring synchrotron radiation sources in the hard X-ray range

O. Chubar

To be published in "ADVANCES IN COMPUTATIONAL METHODS FOR X-RAY OPTICS V"

August 2020

Photon Sciences

Brookhaven National Laboratory

U.S. Department of Energy

USDOE Office of Science (SC), Basic Energy Sciences (BES) (SC-22)

DISCLAIMER

Simulations of coherent scattering experiments at storage ring synchrotron radiation sources in the hard X-ray range

Oleg Chubar*[a], Rebecca Coles[a], Lutz Wiegart[a], Andrei Fluerasu[a], Maksim Rakitin[a], James Condie[a,b], Paul Moeller[c], Rob Nagler[c], Dilip Gersappe[d]
[a]National Synchrotron Light Source II, Brookhaven National Laboratory, NY 11973, USA; [b]University of Nevada, Reno, USA; [c]RadiaSoft LLC, Boulder, CO 80301, USA; [d]Stony Brook University, Stony Brook, NY 11794, USA

ABSTRACT

Detailed simulations of experiments carried out at modern light sources are directly related to the most efficient and productive use of these facilities for research in multiple branches of science and technology. The "Synchrotron Radiation Workshop" computer code with its Python interface, and Sirepo web-browser-based graphical user interface, currently supports physical optics simulations of coherent X-ray scattering and imaging experiments on user-defined virtual samples. We present examples of simulations of coherent scattering experiments that are typically performed at the Coherent Hard X-ray beamline at Brookhaven National Laboratory's (BNL) National Synchrotron Light Source II. We also present several comparisons of the simulations with the results of actual coherent X-ray scattering experiments with nano-fabricated test samples produced at BNL's Center for Functional Nanomaterials.

Keywords: synchrotron radiation, light sources, experiments, coherent X-ray scattering, simulation

1. INTRODUCTION

Detailed and accurate simulation of experiments, being implemented in reliable, available and easy-to-use software, will allow large groups of scientists and engineers to achieve multiple goals related to construction, efficient operation and use of light source facilities for user experiments. For instance, for developers of X-ray beamlines, such capabilities will help to ensure that the beamline design meets all requirements and expectations of its scientific program; for users and scientists supporting operation of a beamline, these will help to test new ideas for experiments, assess technical feasibility of experiments proposed to be carried out at the beamline, determine optimal settings of the beamline transport optics and end-station instrumentation, estimate required detection times and total amount of time required for the experiment, develop and test methods and software for the experimental data processing and interpretation.

Some currently popular and further growing in importance types of experiments, requiring high brightness and coherence of modern light source facilities – low-emittance storage rings and X-ray free electron lasers – can be simulated using the "Synchrotron Radiation Workshop" (SRW), a physical optics computer code for high-accuracy calculation of partially-coherent synchrotron radiation and for simulation of its propagation through optical elements of beamlines [1 - 3]. Among the types of experiments that can be simulated with SRW are coherent scattering, coherent diffractive imaging, and other related techniques. Such simulations can be done with SRW because the interaction of X-ray beam with samples taking place in these experiments can be described by the same of very similar functions / "propagators" that are used in SRW for the physical optics based propagation of the X-rays through optical elements of beamlines. For a fully coherent radiation wavefront described by the frequency-domain electric field, the basic types of such propagators are those extensively used in Fourier optics [4]: the one simulating propagation of the coherent radiation through thin optical elements, consisting in multiplication of the electric field components by a complex transmission function of transverse coordinates, and several others simulating propagation of the electric field in free space between parallel planes, based on one or on two Fast Fourier Transforms (FFTs). E.g. to simulate scattering of coherent X-rays by a thin experimental sample, one can first multiply the incident electric field by the sample's complex transmission, describing absorption and phase shift introduced by the sample, and then use one of the free-space propagators to simulate propagation of this electric field from a plane right after the sample to a detector. In more complicated cases of "thick" samples, in which multiple scattering may take place on electrons with variable density over their volume, one can use combinations of the transmission and free space propagators.

*chubar@bnl.gov; phone 1 631 344-4525

The features of the SRW code supporting partially-coherent calculations [2, 5] can also be easily used for the simulation of experiments with samples illuminated by partially-coherent X-rays [6 - 8]. The main high-accuracy partially-coherent calculation method implemented in SRW for storage ring light sources is based on the summation of contributions from individual (macro-) electrons for calculation of such radiation characteristics as intensity, mutual intensity / cross-spectral density, degree of coherence, mathematical brightness / Wigner distribution. This "summation" means 5-dimensional integration over the phase-space volume of the electron beam, that has to be done "on top" of the integral operations required for the computation of the emission and propagation of each individual electric field [2, 5]. Recent tests and developments of the memory and CPU-efficient coherent mode decomposition [9] algorithms [10] promise to considerably improve feasibility and efficiency of the partially-coherent calculations with SRW code for multiple purposes, including the simulation of experiments for storage ring based light sources. These functionalities seem to be very important, because even in the future ultra-low emittance storage ring based light sources, the emitted radiation will still be only partially coherent in the hard X-ray spectral range [11]. For executing coherence-exploiting experiments at such sources, a compromise will therefore still have to be found between the radiation degree of coherence and the flux at a sample. High-accuracy simulation of such experiments at today's and future light sources will help to do such required optimizations, as well as it will help with other aspects already mentioned above, allowing for the most efficient use of these facilities for science and technology.

In the following sections, we first describe new developments in the Python part of SRW and in the Sirepo web browser based Graphical User Interface (GUI) [12] supporting definition of models of typical experimental samples used in coherent X-ray scattering experiments. We then present examples of simulation of such experiments, using the parameters of the Coherent Hard X-ray (CHX) beamline of the National Synchrotron Light Source II (NSLS-II), from sample models defined using Scanning Electron Microscope (SEM) images of actual nano-samples fabricated at the Center of Functional Nanomaterials (CFN) at BNL, compare the simulated coherent scattering patterns with the corresponding ones measured in experiments at CHX, and also give simulation examples with sample models defined based on geometrical and statistical characteristics.

2. METHODS FOR DEFINING SAMPLES IN SRW AND SIREPO

In the current versions of SRW code and Sirepo web-browser JavaScript GUI, two methods of defining models of experimental samples for the simulation of coherent X-ray scattering and imaging experiments are implemented: a method of defining sample objects from image files (e.g. produced by SEM or simply created in an image editor) and a method of defining samples as 2D (nano-)objects of given shapes randomly distributed over a transverse plane with respect to the optical axis and representing "projection" of a solution with 3D nano-particles on that plane. Examples of using these two methods for defining samples in the Sirepo GUI and in Python interface of SRW are given below.

2.1 Defining samples from image files

The method for defining sample models based on graphical images was implemented in the Python part of SRW and in Sirepo GUI earlier [12], and it has already demonstrated its usefulness for a number of simulations of experiments with SRW [7, 8]. This method makes use of the popular "PIL" Python library [13] for numerical manipulations with image files. Recently, the SRW Python interface and Sirepo GUI were changed, to enable better integration and closer inter-operation of this important method with another method for defining samples, described in the next section, as well as possibly other methods that are expected to be implemented in SRW and in Sirepo in the near future.

The simple steps for defining a sample model from a graphical image file in the new Sirepo GUI are illustrated in figure 1. First, the user has to select a method for defining a sample based on an Image File (see dialog on the left in figure 1). After this, he must select a pre-existing image file, define its possible basic processing parameters (rotation, cropping, interpretation of the grey scale, etc., see dialog in the center in figure 1), resolution (i.e. physical distance between centers of neighboring pixels of the image), maximum thickness and material properties of the sample, based on which the optical path difference and absorption over the sample / image area will be defined. The Sirepo GUI allows to quickly preview the processed image before its final validation and use for creating a transmission object for SRW simulations (see dialog on the right in figure 1). Examples of the coherent X-ray scattering calculations with SRW under Sirepo interface based on SEM images of nano-fabricated samples, and comparisons of these calculations with measurements of the scattering from these samples, performed at the CHX beamline, are presented in section 3.1.

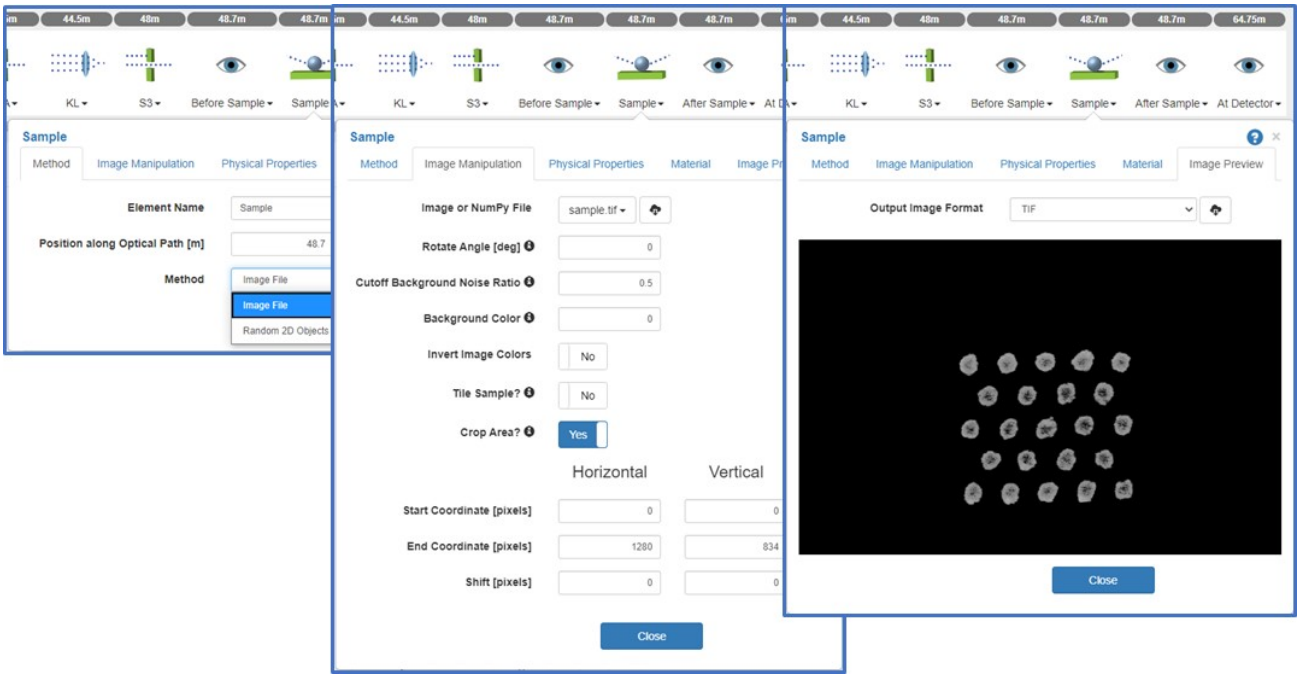

Figure 1. Sirepo GUI dialogs allowing to define models of experimental samples from pre-existing mage files, e.g. those produced by scanning electron microscope. A processed image, that will be used directly for setting up the SRW transmission object for the coherent X-ray scattering simulations, can be quickly previewed in the GUI, as shown on the right.

2.2 Defining samples as randomly-distributed 2D objects

Another method for defining sample models, that was recently implemented in the Python part of SRW and in the Sirepo GUI, is illustrated in figure 2. This method allows to define a model through a set of geometrical and statistical parameters of 2D objects, representing projections of 3D (nano-) objects constituting the sample (e.g. a colloidal solution of nano-particles), on a transverse plane perpendicular to the optical axis of the incident beam. Among possible shapes of the 2D objects are circles, ellipses, triangles, rectangles and higher-order polygons. The objects with non-isotropic shapes can have different ratios of their largest-to-smallest dimensions and can be oriented either strictly along a given direction, or randomly within a range of angles around this direction, according to a given type of distribution. The 2D objects can be distributed randomly over the sample area to reach a specified density, in accordance with a selected distribution type. Figure 2 shows Sirepo GUI dialogs allowing to define these object / sample parameters (see dialog in the middle in figure 2), as well as thickness and material parameters corresponding to the objects, and preview a sample image generated quickly for a given input, before validating it for the use in the coherent scattering simulations.

This sample model definition method is implemented making use of “scikit-image”, an image generation and processing Python library [14]. Thanks to the use of this library and vector operations available in NumPy [15], setting up sample models using this method usually takes seconds. Since sizes of the graphical preview files are usually not very large, iterating on the definition of sample parameters and previewing their auto-generated images in Sirepo also does not require a lot more time, even including the time used for communications between client’s web browser and the Sirepo web server. The definition of the transmission object and performing coherent X-ray scattering calculations with SRW usually takes a bit more time (minutes in the case of fully-coherent simulations). Examples of simulations with sample models defined using this method are given in section 3.2.

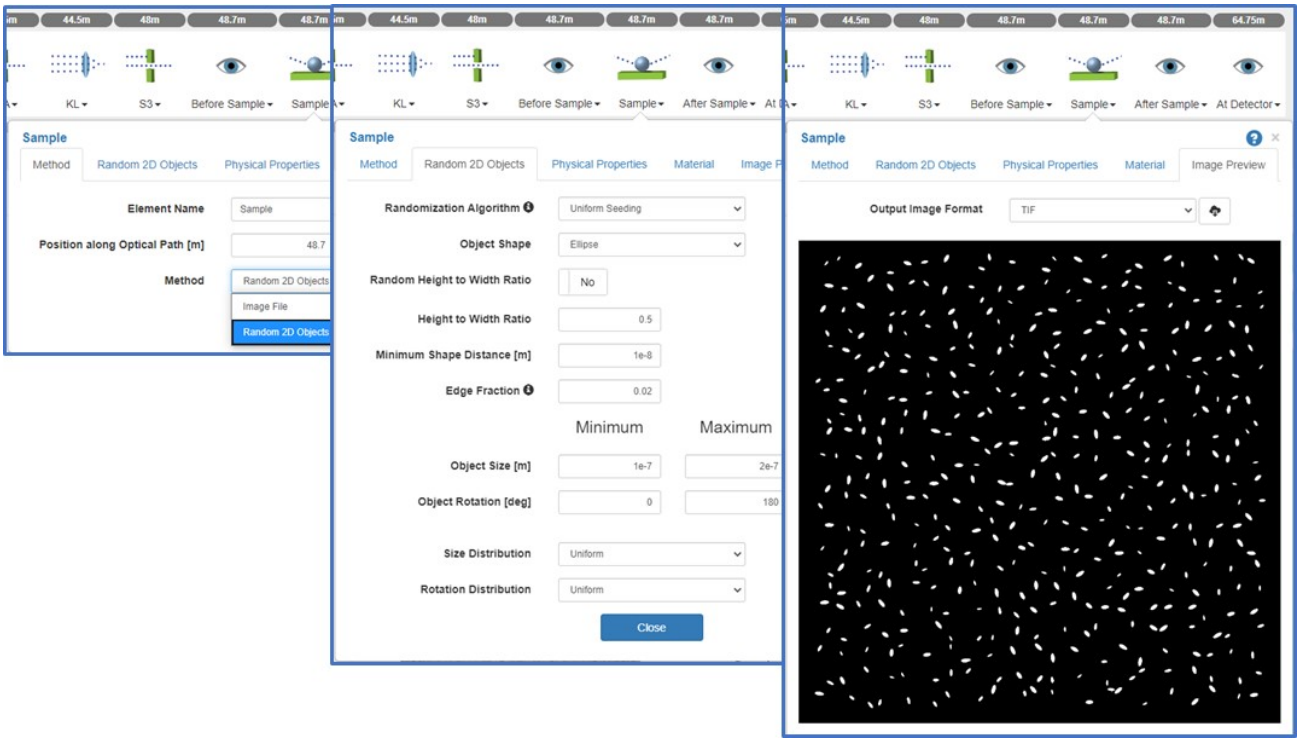

Figure 2. Sirepo GUI dialogs allowing to define models of experimental samples as sets of randomly-distributed 2D objects based on their geometrical and statistical characteristics. An auto-generated preview image, that directly corresponds to the SRW transmission object to be used in the coherent X-ray scattering simulations, can be quickly previewed in the GUI, as shown on the right.

3. EXAMPLES OF COHERENT X-RAY SCATTERING SIMULATIONS WITH DIFFERENT SAMPLE MODELS

After a sample model is defined, using one of the available methods, it can be used in fully- or in partially-coherent simulations of coherent scattering experiments with the SRW code. Such simulations can be done from the Sirepo web interface, benefiting from its direct access to servers or computer clusters, such as NERSC [16]. Alternatively, the simulations can be performed using Python script that can be either generated automatically by Sirepo, or set up manually, by making use of the SRW Python application programming interface, including the functions for defining the sample models. This script can be executed from a command line, in sequential mode for fully-coherent calculations, and either in parallel mode (implemented in SRW using the message passing interface [6]) or in the sequential mode as well for partially-coherent calculation for storage ring based light sources.

3.1 Simulations based on SEM images of nano-fabricated samples, comparison with experimental data

We have performed simulations of coherent X-ray scattering with sample models defined from SEM images of nano-samples manufactured at CFN [17], for the experimental conditions of the CHX beamline [7, 8], with illumination of the samples by partially-coherent X-rays at 9.65 keV photon energy, and compared the results with the experimental data obtained with these samples at the CHX beamline. The results of these simulations and measurements are presented in figure 3, where SEM images of the nano-samples of different geometrical shapes (“dots”, concentric rings, and their combination) are shown on the left, and simulated and measured coherent X-ray scattering patterns in the center and on the right respectively. The distance between the samples and the detector (EIGER 4M with 75 μm square pixel size and 2070 x 2167 numbers of pixels in the horizontal and vertical directions) was ~10 m.

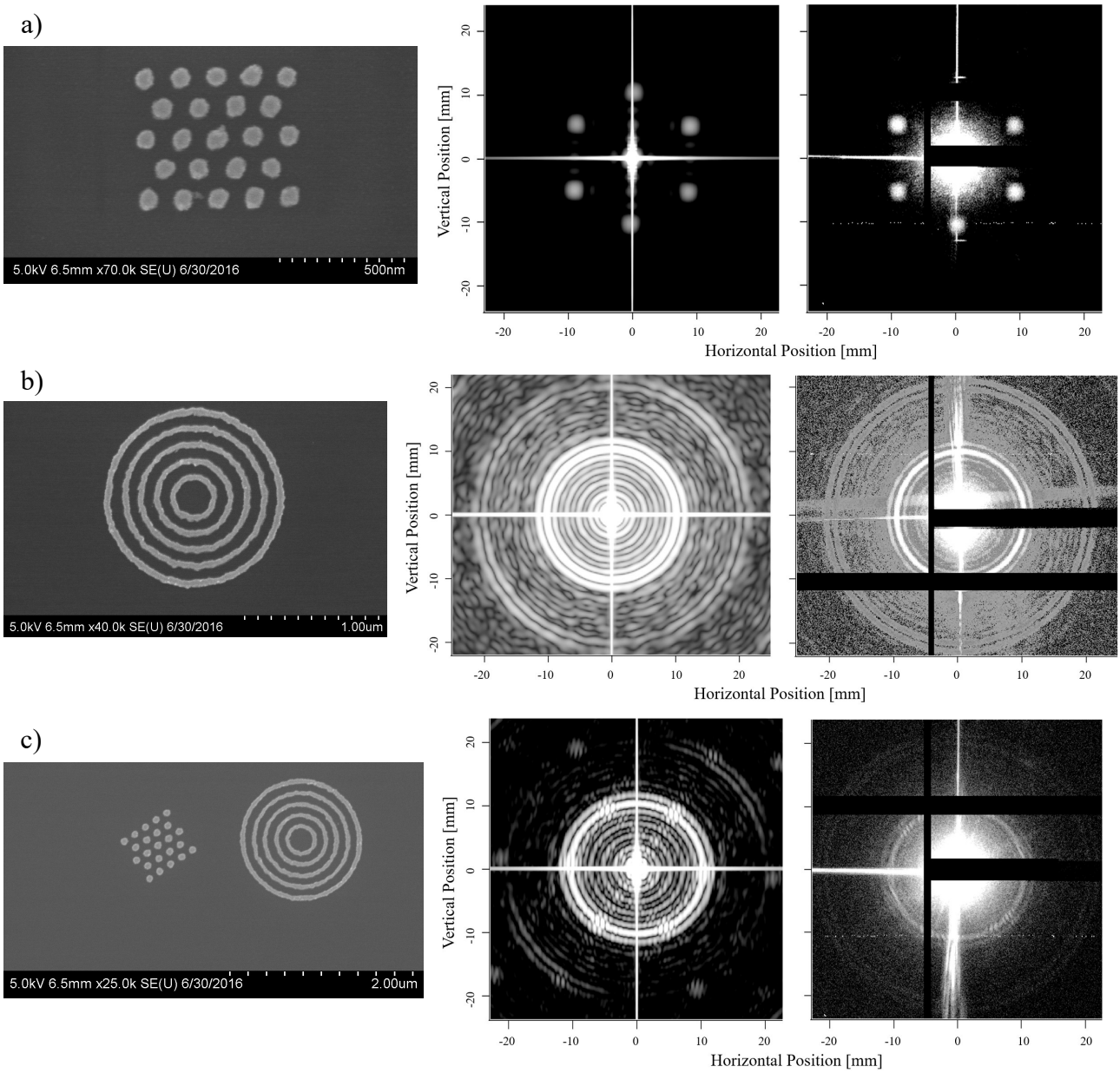

Figure 3. SEM images of nano-samples (left) and the corresponding simulated (center) and measured (right) 9.65 keV coherent X-ray scattering patterns produced by these samples in experiments at the CHX beamline at NSLS-II, for the samples of different geometries: a) regularly placed "dots"; b) concentric rings; c) combinations of "dots" and concentric rings. The scale number in the SEM images corresponds to the distance between left-most and right-most vertical ticks.

One can observe good qualitative agreement between the simulated and measured scattering patterns for each of the samples, strictly corresponding to each sample geometry and its deviations from perfect circular shapes. The white horizontal and vertical lines passing through the centers of all images are due to contribution from slit diffraction (since rectangular slits were limiting the X-ray beam during the measurements). One can notice, however, that in the measured patterns, extra small-angle scattering signal is present (see saturated circular areas in centers of images on the right in figure 3) that can't be seen in the simulations. This can possibly be explained by presence of extra sources of scattering (such as X-ray windows) during the measurements that were not taken into account in the simulations.

3.2 Simulations based on sample models defined by randomly-distributed 2D objects

In many coherent X-ray scattering experiments performed at synchrotron light sources, e.g. X-ray photon correlation spectroscopy experiments, colloidal solutions of nano-particles are used, with the experiments targeting to determine statistical characteristics of spatial and temporal distributions of these nano-particles. If the X-rays' optical path in such a solution is not large, the sample's impact on the radiation can be described within the "thin element" approximation, i.e. by multiplication of the radiation's electric field (corresponding to the emission from an individual macro-electron or representing an independent coherent mode of partially-coherent radiation) by a complex transmission function of transverse coordinates, that can modify both phase and amplitude of the incident electric field, followed by propagation in free space (e.g. to the detector). This transmission can be calculated from the path that is made by an X-ray entering the solution at a given transverse position in the bodies of all nano-objects it crosses in the solution. In a very basic approximation, one can possibly use a distribution of 2D objects of different shapes for the estimation of the optical path: i.e. if ray's transverse position happens to be within area of a 2D object, the radiation at that position gains an optical path difference, that is proportional to some "thickness" parameter (one for all objects). We have added such functionality to SRW and to its web-browser-based interface, Sirepo (see section 2.2), as one of the basic methods for defining sample models for simulating coherent X-ray scattering experiments.

The results of defining 2D randomly-distributed objects of circular and elliptical shapes, and calculation of 9.0 keV coherent X-ray scattering from such sample models, for the conditions of the CHX beamline of NSLS-II, with 16.3 m distance between the sample and observation (detector) plane, are presented in figure 4. We first considered several cases of circles, varying in diameter (see figure 4-a): the case of all circles having 100 nm and 200 nm diameters, and the diameters distributed randomly between these two values (see left, center and right image plots in figure 4-a). For each of the cases, two partially overlapping image plots are shown, one representing the entire sample of 10 x 10 μm^2 in size, and the other showing a 2 x 2 μm^2 detailed view. The calculated scattering patterns (see logarithmic grey-scale image plots in figure 4-b) are strongly dominated by the diffraction on individual circular objects, with smaller-diameter objects producing larger diffraction rings (see main image plot on the left and in the center in figure 4-b). The presence of circular objects with different diameters results in smearing-out of the diffraction pattern (see image plot on the right in figure 4-b). Besides the single-particle diffraction patterns, one can also observe speckle patterns in the coherent X-ray scattering images (see smaller image plot showing 10 x 10 mm^2 sub-area of the total scattering image on the left in figure 4-b) resulting from interference of the radiation scattered by individual nano-objects. Such speckle pattern is present in all scattering image plots shown in figure 4 (see image plots 4-b and 4-d). The sample models defined by randomly-distributed ellipses, all having same dimensions (200 nm size along major and 100 nm along minor axis), are shown in figure 4-c, and their corresponding scattering patterns in figure 4-d. We considered three different cases of orientation of these randomly-distributed ellipses: with all ellipses' major axes oriented at 45º angle with respect to the horizontal / vertical axis (left), with the major axes' angle varying randomly between 15º and 45º (center) and between 0º and 180º (right). As in the examples with circles (figure 4-a, b), the scattering patterns from the elliptical objects are dominated by the diffraction on individual objects (see logarithmic grey-scale image plots in figure 4-d). Note that the pattern obtained for the ellipses oriented randomly within 180º angle (see image plot on the right in figure 4-d) is similar, though more smeared-out, compared to the pattern obtained for the circular objects with the smaller 100 nm diameter (image plot on the left in figure 4-b).

The coherent X-ray scattering calculations illustrated in figure 4 are relatively "memory-hungry": to accurately represent ~100 nm size objects distributed over the ~10 μm range of the entire sample, one may need thousands of data points in the transmission element, and eventually even more, many thousands, of data points in the propagating electric field (in the case where the dimensions of the X-ray beam at the sample are larger than the dimensions of the sample itself). To mitigate memory requirements for storage and numerical manipulations (multiplications and 2D FFTs) with complex data sets representing the electric fields of such wavefronts with many grid points in each of the two transverse directions, we used single-precision numbers for the electric field, and one 2D FFT based free-space propagator (valid within the Fresnel approximation) for simulating the field propagation from the plane right after the sample over a large distance to the detector plane. To ensure numerical efficiency, all the key operations required for such simulations were performed by functions implemented in the C++ part of the SRW code, with the electric field and sample data defined in Python (in arrays supporting buffer interface), and passed "by pointers" to the corresponding functions of the SRW C++ library. Special attention was paid to benchmarking the obtained coherent scattering calculation results vs. those obtained using double-precision data and different, less CPU- and memory-efficient, but eventually more accurate, free-space propagators. The results of these tests demonstrated sufficient accuracy of the single-precision calculations and the one 2D FFT based free-space propagator for the simulation cases illustrated in figure 4.

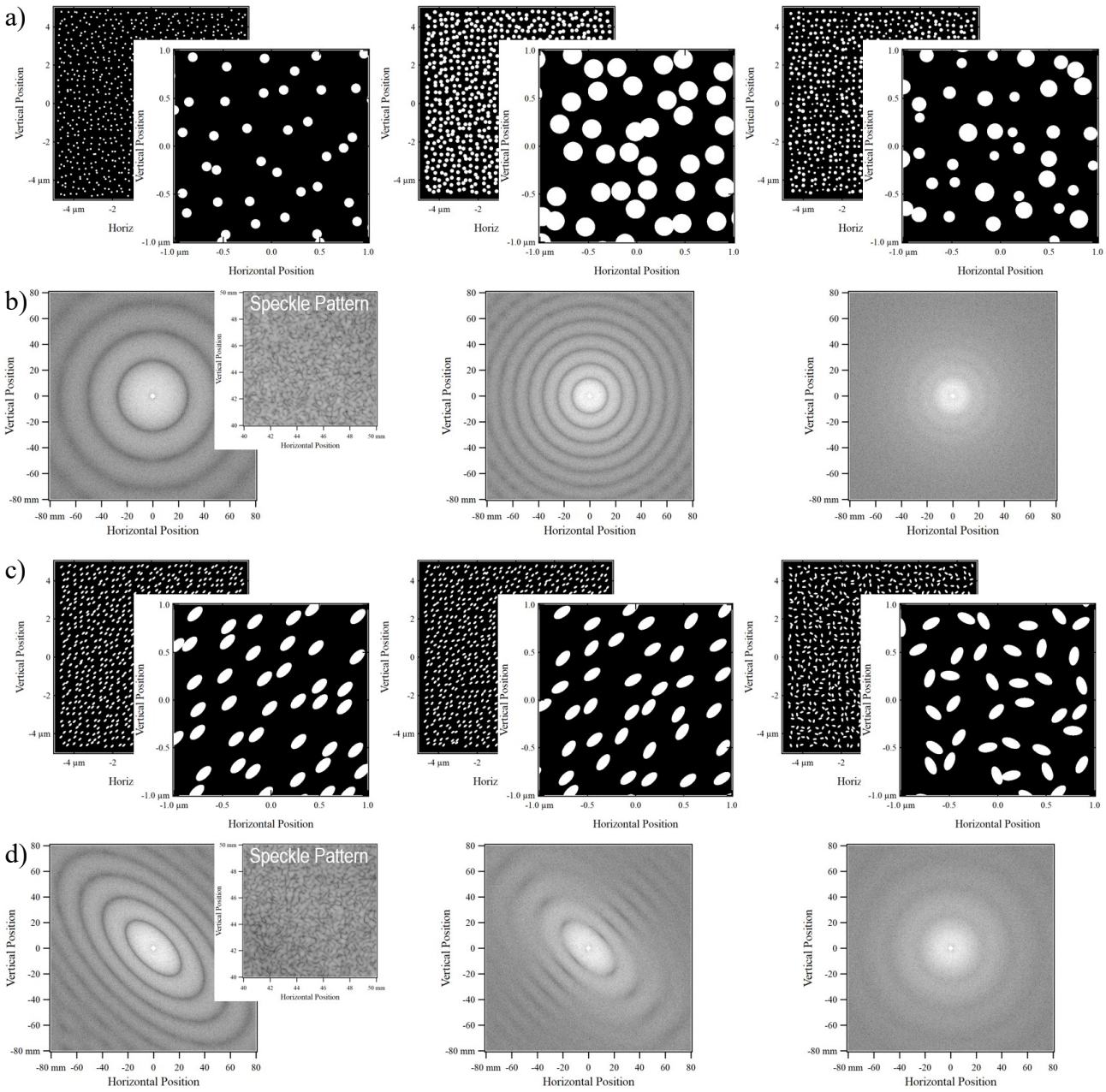

Figure 4. Examples of experimental sample models defined by a set of nanometer-sized randomly-distributed 2D objects (a, c), with two images corresponding to each sample, one for its entire area of 10 x 10 μm^2, and one for a 2 x 2 μm^2 portion of it, and simulated 9.0 keV coherent X-ray scattering patterns created by these samples in the experimental conditions of the CHX beamline (b, d), with each scattering image shown under its corresponding sample image. Zoomed images of the scattering patterns on the left show their speckle structures. The following types of 2D objects were used: a) circles of 100 nm (left) and 200 nm (center) diameter, and diameters randomly distributed between 100 and 200 nm (right); d) ellipses with 200 nm larger and 100 nm smaller dimensions, with their major axes oriented at 45º with respect to the horizontal / vertical axis (left), oriented randomly at different angles between 30º and 60º (center), and between 0º and 180º (right).

4. CONCLUSIONS

We described several updates that were made recently in the SRW physical optics computer code and in its web-browser-based GUI, Sirepo, to support simulation of coherent X-ray scattering experiments – a very important, and still

growing in popularity, type of coherence-exploiting experiments that are carried-out at modern light source facilities. Two different methods are available now for defining sample models for such experiments in SRW / Sirepo – one based on pre-existing images, e.g. generated from SEM measurements, and the other representing samples (e.g. colloidal solutions of nano-particles) by sets of randomly-distributed and randomly-oriented 2D objects. Special attention was paid to validation of the coherent scattering calculation results by experimental data (were available) and by calculations using different methods. We hope to continue these developments in SRW and Sirepo, to further extend the library of functions for defining experimental samples (e.g. to facilitate setting up the colloidal sample models based on 3D nano-objects) and for performing calculations of importance for the simulation of the coherent scattering and other types of experiments, as well as for the processing of experimental data.

ACKNOWLEDGMENTS

We would like to thank Kevin Yager, Julian Lhermitte, Yugang Zhang (CFN, BNL) for manufacturing of nano-samples used in this work, for sharing SEM images describing the samples, and for assistance in development of software functions for sample modeling. The work was supported by DOE BES Field Work Proposal PS-017 and DOE contract DE-SC0012704. This research used the resources of the National Energy Research Scientific Computing Center, a DOE Office of Science User Facility supported by the Office of Science of the US Department of Energy under the Contract No. DE-AC02-05CH11231. We would also like to acknowledge DOE's Science Undergraduate Laboratory Internships program.

REFERENCES

[1] Chubar, O. and Elleaume, P., "Accurate and efficient computation of synchrotron radiation in the near field region", Proc. EPAC-98, 1177-1179 (1998).
[2] Chubar, O., Elleaume, P., Kuznetsov, S., Snigirev, A., "Physical optics computer code optimized for synchrotron radiation", Proc. SPIE 4769, 145 (2002).
[3] https://github.com/ochubar/SRW
[4] Goodman, J. W., Introduction to Fourier Optics, 2nd ed., McGraw-Hill (1996).
[5] Chubar, O. et al., "Development of partially-coherent wavefront propagation simulation methods for 3rd and 4th generation synchrotron radiation sources", Proc. SPIE 8141, 814107 (2011).
[6] Chubar, O., Fluerasu, A., Berman, L., Kaznatcheev, K., Wiegart, L., "Wavefront propagation simulations for beamlines and experiments with 'Synchrotron Radiation Workshop'," J. Phys.: Conf. Ser. 425, 162001 (2013).
[7] Chubar, O., Rakitin, M. S., Chen-Wiegart, Y.-c. K., Fluerasu, A., Wiegart, L., "Simulation of experiments with partially coherent X-rays using Synchrotron Radiation Workshop", Proc. SPIE 10388, 1038811 (2017).
[8] Wiegart, L., Rakitin, M., Zhang, Y. G., Fluerasu, A., Chubar, O., "Towards the Simulation of Partially Coherent X-ray Scattering Experiments", AIP Conference Proceedings 2054, 060079 (2019).
[9] Mandel L. and Wolf E., Optical Coherence and Quantum Optics (Cambridge University Press) 1995.
[10] Li, R., Chubar, O., "CPU and memory efficient coherent mode decomposition for the partially coherent X-ray simulations", these proceedings.
[11] Khubbutdinov, R., Menushenkov, A. P., and Vartanyants, I. A., "Coherence properties of the high-energy fourth-generation X-ray synchrotron sources", J. Synchrotron Rad. 26 (6), 1851-1862 (2019).
[12] Rakitin, M. S. et al., "Sirepo: an open-source cloud-based software interface for X-ray source and optics simulations", J. Synchrotron Rad. 25 1877-1892 (2018).
[13] https://pillow.readthedocs.io
[14] https://scikit-image.org
[15] https://numpy.org
[16] http://www.nersc.gov
[17] Lhermitte, J. R., Stein, A., Tian, C., Zhang, Y., Wiegart, L., Fluerasu, A., Gang, O. & Yager, K. G., "Coherent amplification of X-ray scattering from meso-structures", IUCrJ, 4, 604-613 (2017).